ELSEVIER

Sensors and Actuators B 86 (2002) 49–57

SENSORS AND ACTUATORS B CHEMICAL

www.elsevier.com/locate/sensorb

Asymmetric SPR sensor response curve-fitting equation for the accurate determination of SPR resonance angle

Kazuyoshi Kurihara[a], Kaori Nakamura[b], Koji Suzuki[a,b,*]

[a]*Kanagawa Academy of Science and Technology, 3-2-1 Sakado, Takatsu-ku, Kawasaki 213-0012, Japan*
[b]*Department of Applied Chemistry, Keio University, 3-14-1 Hiyoshi, Kohoku-ku, Yokohama 223-8522, Japan*

Received 27 September 2001; received in revised form 4 March 2002; accepted 19 March 2002

Abstract

An asymmetric surface plasmon resonance sensor response curve (SPR curve) equation derived from the three-layer Fresnel equation regarding p-polarization was proposed that can be used as a more general and appropriate SPR curve equation than Kretschmann's equation given by $R(X) = (1 - \alpha)/\{(X - \beta)^2 + \gamma^2\}$, where R is the reflectance of the incident light, α, β and γ are real parameters, and X the incident angle. The proposed equation is expressed as $R(X) = A[1 - \{B + C(X - D)\}/\{(X - D)^2 + E^2\}]$ with a minimum reflectance at a conventional resonance angle of $X = D + (-B + \sqrt{B^2 + C^2E^2})/C$, where A, B, C, D and E are five real parameters that are very useful as fitting functions for a gold-based SPR curve in real-time measurement. In this equation, a modified resonance angle defined as parameter D is more appropriate than the conventional resonance angle as a variable that gives a linear response to changes in the refractive index of the sensing layer.

Keywords: Surface plasmon resonance; Resonance angle; SPR curve; Real-time measurement

1. Introduction

The surface plasmon resonance (SPR) sensor is a useful analytical tool based on the detection of refractive index changes due to specific adsorption or complexing of the guest target analyte into the host ligand prepared on a metallic film [1,2]. The most popular SPR sensor is commercially available for detecting specific polymers such as proteins concerning antibody–antigen interactions under label-free and real-time conditions [3]. In order to improve the total performance of the SPR sensor for the real-time measurement, reliable and high-speed data analysis is very important.

In typical SPR sensors, the SPR curves of reflectance versus incident light angle are a fundamental concept for analyzing signals caused by the refractive index changes. Kretschmann [4] was the first to provide a theoretical equation of the SPR curve that contains a minimum reflectance whose angle is normally called the resonance angle (RA). According to Kretschmann's theory, SPR signals are obtained by monitoring changes in the RA with some data processing of the SPR curves. Unfortunately, Kretschmann's theoretical equation is roughly approximated from the three-layer Fresnel equation and therefore is not suited for fitting to the SPR curves. The most precise curve-fitting procedure using a multilayer Fresnel equation is acceptable in the static measurement but is much too time-consuming in real-time measurement.

In actual data analysis with SPR curves in real-time measurement, simple methods for finding the RA in the SPR curve are applied such as the quadratic fit, the polynomial fit, the center-of-mass method, the smoothed first-derivative zero-crossing method, and so on. As improved methods, the locally weighted parametric regression (LWPR) method [5,6] and the optimal linear method [7] were proposed. Nevertheless, these methods are just within "minima hunt" techniques in the SPR curve so that useful accurate data for SPR curves situated far from the minimum point corresponding to the RA are not used in these methods. An SPR curve-fitting equation applicable over a wide range around the RA would confer a higher sensitivity to the real-time SPR sensors.

We now propose a new SPR curve-fitting equation for real-time measurement that fits much better to almost all the SPR curves experimentally obtained. The new equation is applicable to asymmetric SPR curves frequently obtained with a gold (Au)-based SPR sensor. Our asymmetric SPR curve-fitting equation was derived by closer approximation of the three-layer Fresnel equation relating to p-polarization

* Corresponding author. Present address: Department of Applied Chemistry, Keio University, 3-14-1 Hiyoshi, Kohoku-ku, Yokohama 223-8522, Japan. Fax: +81-45-564-5095.
E-mail address: suzuki@applc.keio.ac.jp (K. Suzuki).

0925-4005/02/$ – see front matter
PII: S0925-4005(02)00146-6

than Kretschmann's SPR curve equation. Interestingly, we have theoretically found that the conventional RA that gives the minimum peak in the SPR curves is not the most appropriate variable to monitor linear changes in refractive index but is only an approximate one. A modified RA defined by parameter D in the asymmetric SPR curve-fitting equation is the most suitable variable for the SPR analysis. The effectiveness of the proposed curve-fitting equation was estimated by numerical calculations using actual optical parameters and was demonstrated by Au-based SPR sensor experiments with sucrose solutions.

2. Theory

We assumed a simple SPR sensory system which consists of three layers of a prism–metal–sensing layer structure with a Kretschmann attenuated total reflection (ATR) configuration as shown in Fig. 1. A glass prism, a metallic film, and a sensing layer are abbreviated to p, m and s, respectively. When the p-polarized light has an incident angle θ in units of radians, the reflectance R of the light is given by the three-layer Fresnel equation relating to p-polarization as follows [8–10]:

$$R = |r_{\mathrm{pms}}|^2 \tag{1}$$

with

$$r_{\mathrm{pms}} = \frac{r_{\mathrm{pm}} + r_{\mathrm{ms}} \exp(2\mathrm{i}k_{\mathrm{mz}}d)}{1 + r_{\mathrm{pm}} r_{\mathrm{ms}} \exp(2\mathrm{i}k_{\mathrm{mz}}d)} \tag{2}$$

$$r_{\mathrm{pm}} = \frac{k_{\mathrm{pz}}\varepsilon_{\mathrm{m}} - k_{\mathrm{mz}}\varepsilon_{\mathrm{p}}}{k_{\mathrm{pz}}\varepsilon_{\mathrm{m}} + k_{\mathrm{mz}}\varepsilon_{\mathrm{p}}} \tag{3}$$

$$r_{\mathrm{ms}} = \frac{k_{\mathrm{mz}}\varepsilon_{\mathrm{s}} - k_{\mathrm{sz}}\varepsilon_{\mathrm{m}}}{k_{\mathrm{mz}}\varepsilon_{\mathrm{s}} + k_{\mathrm{sz}}\varepsilon_{\mathrm{m}}} \tag{4}$$

and

$$k_{jz} = \left(\varepsilon_j \frac{\omega^2}{c^2} - k_x^2\right)^{1/2} \quad \text{for } j = \mathrm{p, m, s} \tag{5}$$

$$k_x = \sqrt{\varepsilon_{\mathrm{p}}}\frac{\omega}{c}\sin\theta \tag{6}$$

$$\omega = \frac{2\pi c}{\lambda} \tag{7}$$

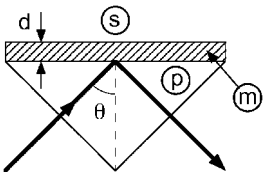

Fig. 1. A Kretschmann configuration of a prism–metal–sensing layer interface. The glass prism, the metallic film and the sensing layer are labeled p, m and s, respectively. θ is the incident angle while d is the thickness of the metallic film.

where r_{pm} and r_{ms} are the amplitude reflectances given by the Fresnel formula relating to p-polarization for prism–metal and metal–sensing layer interfaces, respectively, ε_j and k_{jz} are the dielectric constant and the wave-vector component perpendicular to the interface in medium j, respectively, k_x the component of the incident wave-vector parallel to the interface, given as a real number, d the thickness of the metallic film, ω and λ are the angular frequency and the wavelength of the incident light, respectively, and c the velocity of light.

The complex wavenumber k_0 of the surface plasmon wave generated at the metal–sensing layer interface in the absence of the prism is derived from the following equation [1] with the variable parameter k_x:

$$k_{\mathrm{mz}}\varepsilon_{\mathrm{s}} + k_{\mathrm{sz}}\varepsilon_{\mathrm{m}} = 0 \tag{8}$$

where k_0 is then obtained by

$$k_0 = \frac{\omega}{c}\left(\frac{\varepsilon_{\mathrm{m}}\varepsilon_{\mathrm{s}}}{\varepsilon_{\mathrm{m}} + \varepsilon_{\mathrm{s}}}\right)^{1/2} \tag{9}$$

In the simplest approximation, the SPR phenomenon strongly occurs when the variable parameter k_x is equal to k_0. Because the value of r_{ms} becomes an anomaly when $k_x = k_0$, Eq. (2) can be transferred as follows:

$$\begin{aligned} r_{\mathrm{pms}}(k_x) &= \frac{1 + r_{\mathrm{ms}} r_{\mathrm{pm}}^{-1} \exp(2\mathrm{i}k_{\mathrm{mz}}d)}{1 + r_{\mathrm{ms}} r_{\mathrm{pm}} \exp(2\mathrm{i}k_{\mathrm{mz}}d)} r_{\mathrm{pm}} \\ &= \frac{f(k_x) + g(k_x) r_{\mathrm{pm}}^{-1} \exp(2\mathrm{i}k_{\mathrm{mz}}d)}{f(k_x) + g(k_x) r_{\mathrm{pm}} \exp(2\mathrm{i}k_{\mathrm{mz}}d)} r_{\mathrm{pm}} \end{aligned} \tag{10}$$

with

$$f(k_x) = k_{\mathrm{mz}}\varepsilon_{\mathrm{s}} + k_{\mathrm{sz}}\varepsilon_{\mathrm{m}} \tag{11}$$

and

$$g(k_x) = k_{\mathrm{mz}}\varepsilon_{\mathrm{s}} - k_{\mathrm{sz}}\varepsilon_{\mathrm{m}} \tag{12}$$

Here, the function $f(k_x)$ is applied to a Taylor expansion at $k_x = k_0$ while $g(k_x)$, r_{pm} and k_{mz} are approximated as $g(k_0)$, $(r_{\mathrm{pm}})_{k_x=k_0}$ and $(k_{\mathrm{mz}})_{k_x=k_0}$ at $k_x = k_0$, respectively, and the following equations are then obtained:

$$f(k_x) \cong f(k_0) + f'(k_0)(k_x - k_0) = -\frac{\varepsilon_{\mathrm{m}}^2 - \varepsilon_{\mathrm{s}}^2}{\sqrt{\varepsilon_{\mathrm{m}}\varepsilon_{\mathrm{s}}}}(k_x - k_0) \tag{13}$$

$$g(k_x) \cong g(k_0) = -\frac{\omega}{c}\frac{2\varepsilon_{\mathrm{m}}\varepsilon_{\mathrm{s}}}{\sqrt{\varepsilon_{\mathrm{m}} + \varepsilon_{\mathrm{s}}}} \tag{14}$$

$$r_{\mathrm{pm}} \cong (r_{\mathrm{pm}})_{k_x=k_0} = \frac{\sqrt{\varepsilon_{\mathrm{p}}(\varepsilon_{\mathrm{m}} + \varepsilon_{\mathrm{s}}) - \varepsilon_{\mathrm{m}}\varepsilon_{\mathrm{s}}} + \varepsilon_{\mathrm{p}}}{\sqrt{\varepsilon_{\mathrm{p}}(\varepsilon_{\mathrm{m}} + \varepsilon_{\mathrm{s}}) - \varepsilon_{\mathrm{m}}\varepsilon_{\mathrm{s}}} - \varepsilon_{\mathrm{p}}} \tag{15}$$

and

$$k_{\mathrm{mz}} \cong (k_{\mathrm{mz}})_{k_x=k_0} = -\frac{\omega}{c}\frac{\varepsilon_{\mathrm{m}}}{\sqrt{\varepsilon_{\mathrm{m}} + \varepsilon_{\mathrm{s}}}} \tag{16}$$

These four equations, Eqs. (13)–(16), make Eq. (10) a simple equation as follows:

$$r_{\mathrm{pms}}(k_x) \cong \frac{k_x - k_0 - \rho\sigma^{-1}}{k_x - k_0 - \rho\sigma}\sigma = \frac{k_x - k_0 - \sigma^{-2}k_{\mathrm{R}}}{k_x - k_0 - k_{\mathrm{R}}}\sigma \tag{17}$$

with

$$\rho \equiv -\frac{\omega}{c}\left(\frac{2}{\varepsilon_{\mathrm{m}} - \varepsilon_{\mathrm{s}}}\right)\left(\frac{\varepsilon_{\mathrm{m}}\varepsilon_{\mathrm{s}}}{\varepsilon_{\mathrm{m}} + \varepsilon_{\mathrm{s}}}\right)^{3/2} \exp\left[i\frac{4\pi d}{\lambda}\frac{\varepsilon_{\mathrm{m}}}{(\varepsilon_{\mathrm{m}} + \varepsilon_{\mathrm{s}})^{1/2}}\right] \tag{18}$$

$$\sigma \equiv [r_{\mathrm{pm}}]_{k_x = k_0} \tag{19}$$

and

$$k_{\mathrm{R}} \equiv \rho\sigma \tag{20}$$

where k_{R} is the perturbation of k_0 in the presence of the prism. Surface plasmon waves in the Kretschmann configuration have the complex wavenumber k_{SP} given by

$$k_{\mathrm{SP}} = k_0 + k_{\mathrm{R}} \tag{21}$$

Eq. (17) is a fundamental equation when the SPR curves are discussed. In the approximation that leads to the symmetric SPR curve equation given by Kretschmann, two conditions are assumed as follows:

$$\sigma \cong \exp[\mathrm{i}\phi] \tag{22}$$

and

$$|\rho''| \ll |\rho'| \tag{23}$$

where ϕ is a real number. Under these two conditions of Eqs. (22) and (23), the term $\rho\sigma^{-1}$ can be described as follows:

$$\rho\sigma^{-1} \cong k_{\mathrm{R}}^{*} \tag{24}$$

where k_{R}^{*} is the complex conjugate of k_{R}. By substituting Eqs. (20) and (24) into the second term in Eq. (17), we finally obtain the symmetric SPR curve equation as follows:

$$R = |r_{\mathrm{pms}}(k_x)|^2 \cong \left|\frac{k_x - k_0 - k_{\mathrm{R}}^{*}}{k_x - k_0 - k_{\mathrm{R}}}\exp[\mathrm{i}\phi]\right|^2 = 1 - \frac{\alpha}{(k_x - \beta)^2 + \gamma^2} \tag{25}$$

with

$$\alpha \equiv 4k_0'k_{\mathrm{R}}'' \tag{26}$$

$$\beta \equiv k_0' + k_{\mathrm{R}}' = k_{\mathrm{SP}}' \tag{27}$$

and

$$\gamma \equiv k_0'' + k_{\mathrm{R}}'' = k_{\mathrm{SP}}'' \tag{28}$$

where the mathematical descriptions of x' and x'' mean the real and imaginary parts of the complex number x, respectively. The SPR curves in Eq. (25) are symmetrical to the axis of $k_x = k_{\mathrm{SP}}'$ because the equation contains only a quadratic term of $(k_x - k_{\mathrm{SP}}')$.

In our case, no condition is imposed in Eq. (17), which can be exactly transferred to the following equation with five real parameters of A, B, C, D and E:

$$R = |r_{\mathrm{pms}}(k_x)|^2 \cong \left|\frac{k_x - k_0 - \sigma^{-2}k_{\mathrm{R}}}{k_x - k_0 - k_{\mathrm{R}}}\sigma\right|^2 = A\left(1 - \frac{B + C(k_x - D)}{(k_x - D)^2 + E^2}\right) \tag{29}$$

with

$$A \equiv \left|\frac{1}{\sqrt{s}}\right|^2 \tag{30}$$

$$B \equiv (2s' - 1)k_{\mathrm{R}}'^2 + k_{\mathrm{R}}''^2 - 2s''k_{\mathrm{R}}'k_{\mathrm{R}}'' - 2s''k_0''k_{\mathrm{R}}' + 2(1 - s')k_0''k_{\mathrm{R}}'' - |s|^2|k_{\mathrm{R}}|^2 \tag{31}$$

$$C \equiv 2\{(s' - 1)k_{\mathrm{R}}' - s''k_{\mathrm{R}}''\} \tag{32}$$

$$D \equiv k_{\mathrm{SP}}'(= k_0' + k_{\mathrm{R}}') \tag{33}$$

$$E \equiv k_{\mathrm{SP}}''(= k_0'' + k_{\mathrm{R}}'') \tag{34}$$

and

$$s \equiv \sigma^{-2} \tag{35}$$

where we define the value of s as the characteristic factor of the asymmetric SPR curves. The meaning of the parameters in Eq. (29) for the SPR curves are: A gives the maximum value of the SPR curves, B and C contribute to the symmetry and asymmetry of the SPR curves, respectively, D is a modified RA that is the most appropriate variable that monitors changes in the refractive index, and E is the imaginary part of the complex wavenumber of surface plasmon waves in the Kretschmann configuration and is related to the dip-width of SPR curves. Compared with Kretschmann's equation of Eq. (25), our equation (Eq. (29)) is not symmetrical to the axis of $k_x = k_{\mathrm{SP}}'$ because our equation contains the linear term of $(k_x - k_{\mathrm{SP}}')$. Eq. (29) is more general and appropriate than Kretschmann's equation because we impose no condition on the fundamental equation (Eq. (17)); thus the equation is more suitable for a fitting function.

In Eq. (29), the reflectance has a dip at a conventional RA θ_{min} and a minimum reflectance R_{min} given by

$$n_{\mathrm{p}}\frac{\omega}{c}\sin\theta_{\mathrm{min}} = D + \frac{-B + \sqrt{B^2 + C^2E^2}}{C} \cong D \tag{36}$$

$$R_{\mathrm{min}} = A\left(1 - \frac{B + \sqrt{B^2 + C^2E^2}}{2E^2}\right) \cong A\left(1 - \frac{B}{E^2}\right) \tag{37}$$

with

$$n_{\mathrm{p}} = \sqrt{\varepsilon_{\mathrm{p}}} \tag{38}$$

where n_{p} is the refractive index of the prism; the approximations indicated by '≅' in Eqs. (36) and (37) are obtained under the condition of $B \gg CE(> 0)$.

The principle of SPR analysis is based on the momentum conservation in the real part between the evanescent wave and the surface plasmon wave given by

$$k_x = k'_{\mathrm{SP}} \tag{39}$$

where k_x denotes the wavenumber of the evanescent wave generated by the incident light and k'_{SP} denotes the real part of the complex wavenumber of the surface plasmon wave. Eq. (39) determines the specific angle θ_{SPR} given by

$$n_{\mathrm{p}} \frac{\omega}{c} \sin\theta_{\mathrm{SPR}} = k'_0 + k'_{\mathrm{R}} \tag{40}$$

Thus, one can measure changes in the refractive index of the sensing layer on the basis of the following useful formula that is an approximation of Eq. (40):

$$\sin\theta_{\mathrm{SPR}} \cong \frac{n_{\mathrm{s}}}{n_{\mathrm{p}}} \tag{41}$$

with

$$n_{\mathrm{s}} = \sqrt{\varepsilon_{\mathrm{s}}} \tag{42}$$

where n_{s} is the refractive index of the sensing layer. In Kretschmann's approximate equation (Eq. (25)), the angle θ_{SPR} is the conventional RA, because it makes the reflectance a minimum in Eq. (25). However, in our asymmetric equation (Eq. (29)), because the conventional RA presenting the minimum reflectance, θ_{min}, is given by Eq. (36), the angle θ_{SPR} is not the conventional RA, θ_{min}. We call the angle θ_{SPR} a modified RA in our asymmetric SPR equation as a distinction from the conventional RA, θ_{min}, that presents the minimum reflectance. In a physical phenomenon, θ_{SPR} and θ_{min} are determined by the momentum conservation in the real part and in the complex, respectively, between the evanescent wave and the surface plasmon wave. The modified RA, θ_{SPR}, is more suitable than the conventional RA, θ_{min}, for measuring linear changes in the refractive index, because the useful formula in Eq. (41) is a good approximation of θ_{SPR} rather than θ_{min}. This is a new concept for the SPR curve data analysis.

3. Numerical procedure

Numerical calculations were carried out using two software programs, Mathematica 4 (Wolfram Research) and Igor Pro (Wave Metrics). The numerical data for theoretical SPR curves obtained by the Mathematica calculations were fitted to our asymmetric SPR curve equation using a curve-fitting routine of Igor Pro. The curve-fitting operation using Igor Pro is designed for user-defined fits that allow one to define the fitting function, the weighting for each point and the epsilon values to calculate the partial derivatives with respect to each coefficient. Igor Pro uses the Levenberg–Marquardt algorithm [11] that is a standard resolution of the problem to search for the coefficient values in the nonlinear least-squares method. In all the fits, the weighting and the epsilon values were automatically selected according to the user's manual for Igor Pro. The weighting is unity for all the raw data while the epsilon values for each coefficient, K, are $10^{-10} \times K$.

4. Experimental

In the SPR sensor response experiments, the refractive indices of the sucrose solutions with five concentrations of 0, 1, 4, 10 and 20 wt.% were basically measured with a commercial SPR instrument (DKK, Japan), which is flexible in the optical elements such as a prism and a light source. The optical system was the typical Kretschmann ATR configuration. The prism was a hemicylindrical prism made from SFL6 glass (OHARA, Tokyo, Japan) with a high refractive index of 1.80 at 587 nm. The light source was two light-emitting diodes (LEDs) that had central wavelengths of ∼630 and ∼880 nm with half widths of ∼20 and ∼40 nm, respectively. The light was focused into a converging beam through a cylindrical lens so that the sensor surface was simultaneously observed over a range of incident angles. A charge-coupled device (CCD; SONY XC-77, Tokyo, Japan) was used to measure the reflected light intensity as a function of the incident angle. A linear polarizer was placed between the prism and the CCD to selectively observe the reflected light of the p- or s-polarizations. The SPR curve was obtained by dividing the reflected light intensity of the p-polarization by that of the s-polarization because the non-homogeneous distribution of the light intensity was removed.

The gold substrates for the SPR experiments had a 45 nm thick gold film with an area of 20 × 20 mm deposited onto 51 mm × 20 mm × 1 mm thick SFL6 glass plates. A 5 nm thick layer of chromium was placed between the gold film and the glass plate to improve the adhesion of the gold to the glass. A minimum amount of matching fluid was used to reduce the reflection at the glass surfaces when the gold substrate was fixed to the hemicylindrical prism.

5. Results and discussion

The asymmetric SPR curve equation given by Eq. (29) was examined for its effectiveness as an approximate equation using numerical calculations and for its usefulness as a fitting function using actual SPR experiments. In the SPR numerical simulations, the refractive index of a water solution was measured by an Au-based SPR sensor with a prism having a high refractive index, $n_{\mathrm{p}} = 1.80$. The typical refractive index of water, n_{w}, is given by $n_{\mathrm{w}} = 1.3330$ at a wavelength of 589.3 nm and a temperature of 20 °C. The dispersion effect is included in the gold metal, but not in the prism and the water solutions. As dispersive optical

parameters of Au, the Drude model was assumed for the dielectric constant of the metal layer, ε_m, as

$$\varepsilon_m = \varepsilon_m^\infty - \frac{\omega_p^2}{\omega(\omega + i\omega_\tau)} \quad (43)$$

where ω_p and ω_τ are the plasma frequency and the damping frequency, respectively, ε_m^∞ is the background frequency of the metal at a frequency of infinity. According to the curve-fitting of reliable data in the literature [12], the following values can be used: $\varepsilon_m^\infty = 9.75$, $\omega_p = 1.36 \times 10^{16}$ rad/s and $\omega_\tau = 1.45 \times 10^{14}$ rad/s in the range 600–900 nm.

In Figs. 2 and 3, the asymmetric SPR curve equation from Eq. (29) was examined at wavelengths of 600 and 800 nm, respectively. In part (a) of Figs. 2 and 3, the solid lines represent the original SPR curves obtained by the three-layer Fresnel equation of p-polarization while the broken lines are the SPR curves obtained by the asymmetric SPR curve equation of approximation using Eqs. (29)–(35). The SPR curves were measured with five different metallic thicknesses of 30, 40, 50, 60 and 70 nm. The approximate SPR curves denoted by the broken lines correspond well with the original SPR curves indicated by the solid line when the metallic thickness is 50, 60 and 70 nm in Fig. 2 and 40, 50, 60 and 70 nm in Fig. 3. The approximate SPR curves agree closely but not exactly with the original SPR curves. In part (b) of Figs. 2 and 3, the original SPR curves denoted by the solid lines were fitted to the asymmetric SPR curve equation with five parameters A, B, C, D and E in Eq. (29). The fits were done in the range 10° from 52° to 62° in Fig. 2b and from 48° to 58° in Fig. 3b. The fitting curves denoted by the broken lines cannot be seen in these figures because of the very good agreement between the fitting curves and the original SPR curves. This indicates that the asymmetric SPR curve equation is very useful as a fitting function of the SPR curve. Part (c) of Figs. 2 and 3 shows the ratios of the five parameters A–E obtained by the fitting procedures to those given by Eqs. (30)–(34) in the asymmetric SPR curve

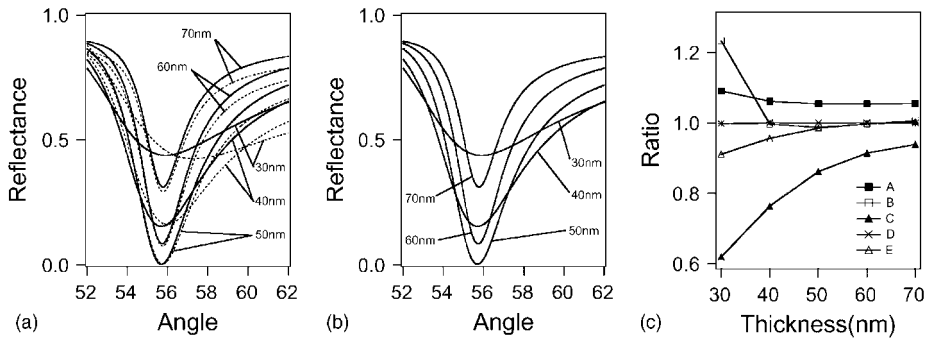

Fig. 2. Numerical calculations of asymmetric SPR curve equation at an excitation wavelength of 600 nm. It is assumed that water with a refractive index of 1.3330 is measured by an Au-based SPR with the prism having a high refractive index of 1.80: (a) SPR curve comparison of the asymmetric SPR curve equation of Eq. (29) (broken line) with the complete equation given by the three-layer Fresnel equation of p-polarization (solid line). Five SPR curves with Au-film thicknesses of 30, 40, 50, 60 and 70 nm are compared; (b) SPR curves (solid line) obtained by the complete equation are fitted to asymmetric SPR curve equation of Eq. (29) with unknown parameters A, B, C, D and E; (c) ratios of five parameters A, B, C, D and E obtained by the fitting procedure to those given by Eqs. (30)–(35) in the asymmetric SPR curve equation (parameter D is unity with an error of 0.2%).

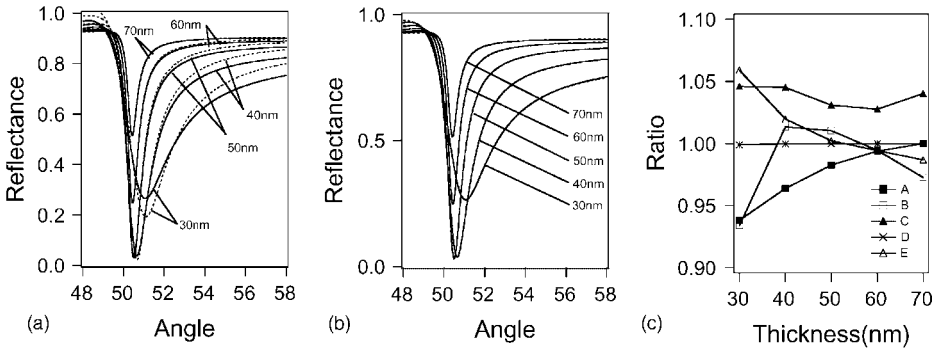

Fig. 3. Numerical calculations of asymmetric SPR curve equation at an excitation wavelength of 800 nm. Numerical values for calculations are the same as those used in Fig. 2 except for the excitation wavelength: (a) SPR curve comparison of the asymmetric SPR curve equation of Eq. (29) (broken line) with the complete equation given by three-layer Fresnel equation of p-polarization (solid line); (b) SPR curves (solid line) obtained by the complete equation are fitted to the asymmetric SPR curve equation of Eq. (29); (c) ratios of five parameters A, B, C, D and E obtained by the fitting procedure to those given by Eqs. (30)–(35) in the asymmetric SPR curve equation (parameter D is unity with an error of 0.2%).

equation. Of five parameters, only parameter D is unity within an error of about 0.2%. Parameter D is especially important in the SPR experiments because it is the modified RA that provides correct information on linear changes in the refractive index of the sensing layer. The exact agreement in parameter D between the theory and the fitting means that the approximation is highly effective and also shows that the asymmetric SPR curve equation of Eq. (29) is useful as a fitting function.

In the actual SPR experiments, the real-time change in the reflectance dip in the SPR curves is monitored in which the relative but not the absolute measurements of the angle are normally carried out. In this case, the asymmetric SPR curve equation given by Eq. (29) is unsuitable for numerical calculations in data processing because some information on the absolute value of the incident angle θ is necessary. This problem can be resolved by applying the function $k_x(\theta)$ to the first-order expansion of a Taylor series at $\theta = \theta_{SPR}$ as follows:

$$k_x(\theta) \cong \sqrt{\varepsilon_p}\frac{\omega}{c}\{\sin\theta_{SPR} + (\theta - \theta_{SPR})\cos\theta_{SPR}\} \tag{44}$$

Using this equation, the asymmetric SPR curve equation of Eq. (29) is further transferred to the following equation:

$$R(X) \cong A\left(1 - \frac{B + C(X - D)}{(X - D)^2 + E^2}\right) \tag{45}$$

where X is the incident angle; the replacements are given by $A \Rightarrow A$, $\Lambda^2 B \Rightarrow B$, $\Lambda C \Rightarrow C$, $\theta_{SPR} - \sin\theta_{SPR} + \Lambda D \Rightarrow D$, $\Lambda E \Rightarrow E$ and $\theta \Rightarrow X$ with $\Lambda = c/\omega\sqrt{\varepsilon_p}$. When the unit of X is degrees, the replacements are given by $A \Rightarrow A$, $\Lambda^2 B \Rightarrow B$, $\Lambda C \Rightarrow C$, $(180/\pi)(\theta_{SPR} - \sin(\pi/180)\theta_{SPR}) + \Lambda D \Rightarrow D$, $\Lambda E \Rightarrow E$, $(180/\pi)\theta \Rightarrow X$ with $\Lambda = (180/\pi)c/\omega\sqrt{\varepsilon_p}$. As referred to in Eqs. (36) and (37), the $R(X)$ of Eq. (45) has a minimum, R_{min}, at $X = X_{min}$ given by

$$R_{min}(X_{min}) = A\left(1 - \frac{B + \sqrt{B^2 + C^2E^2}}{2E^2}\right) \tag{46}$$

and

$$X_{min} = D + \frac{-B + \sqrt{B^2 + C^2E^2}}{C} \tag{47}$$

When these procedures are applied to Eq. (25), Eq. (48) can be obtained:

$$R_K(X) \cong 1 - \frac{\alpha}{(X - \beta)^2 + \gamma^2} \tag{48}$$

where X is the incident angle; descriptions of the replacements are omitted here. This is a fitting function of Kretschmann's SPR equation for the actual experiments.

In Figs. 4 and 5, the usefulness of the asymmetric SPR curve equation of Eq. (45) as a fitting function for SPR curves is assessed. As the original SPR curves were fitted to the asymmetric SPR curve equation, we used SPR curves calculated by the three-layer Fresnel equation relating to the p-polarization at the excitation wavelengths of 600 and 800 nm in Figs. 4 and 5, respectively. In the calculations, water solutions with refractive indexes of 1.333–1.368 by 0.005 increments were used that were obtained with the Au-based SPR sensor that had an Au-film thickness of 50 nm and a prism with a refractive index of 1.80. In part (a) of Figs. 4 and 5, the original SPR curves are indicated by the solid lines while the fitting SPR curves are shown by the broken lines. The fits were also done in a range of 10° from 52° to 62° in Fig. 4a and from 48° to 58° in Fig. 5a. The fitting curves are hardly seen in these figures because the original curves and the fitting curves almost overlapped. Part

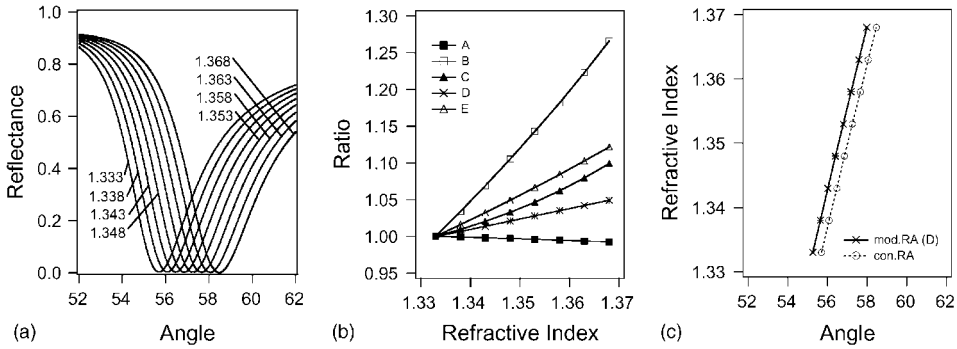

Fig. 4. Curve-fitting to the asymmetric SPR curve equation when the original SPR curves are calculated at an excitation wavelength of 600 nm by the three-layer Fresnel equation relating to p-polarization. It is assumed that water solutions with refractive indices of 1.333–1.368 by 0.005 increment are measured by an Au-based SPR that has an Au-film thickness of 50 nm and a prism refractive index of 1.80. (a) Calculated SPR curves indicated by solid lines are fitted to the asymmetric SPR curve equation whose curves are shown by broken lines but are hardly seen because the original curves cover the fitting curves. (b) Dependence of the fitting parameters A, B, C, D and E on the refractive index of the sensing layer. The fitting parameters are, respectively, normalized by those obtained when the refractive index in the sensing layer is 1.333 as shown in Table 1. (c) Responses to refractive index changes in the modified resonance angle (mod.RA) defined as parameter D and the conventional resonance angle (con.RA) that precisely gives the minimum point in the reflectance. The con.RA is described as $D + (-B + \sqrt{B^2 + C^2E^2})/C$ in Eq. (47).

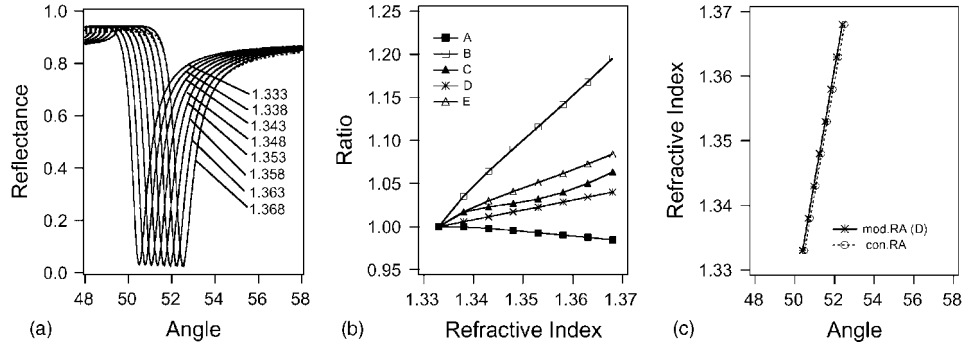

Fig. 5. Curve-fitting to the asymmetric SPR curve equation when the original SPR curves are calculated at an excitation wavelength of 800 nm. Numerical calculations are the same as those used in Fig. 4 except for the excitation wavelength: (a) Calculated SPR curves indicated by solid lines are fitted to the asymmetric SPR curve equation whose curves are shown by a broken line; (b) Dependence of the fitting parameters A, B, C, D and E on the refractive index of the sensing layer. The fitting parameters are, respectively, normalized by those obtained when the refractive index in the sensing layer is 1.333 as shown in Table 1. (c) Responses to refractive index changes in the mod.RA and con.RA.

(b) of Figs. 4 and 5 shows the dependence of the fitting parameters A, B, C, D and E on the refractive index of the sensing layer. These five fitting parameters were, respectively, normalized by those obtained when the refractive index in the sensing layer is 1.333 as shown in Table 1. The parameters with a linear correlation coefficient, r, of $1 - |r| < 10^{-3}$ are A, D and E in Fig. 4b, and D in Fig. 5b. The linear correlation coefficients of A, B, C, D and E in Figs. 4b and 5b are summarized in Table 2. Only parameter D satisfies the condition of $1 - |r| < 10^{-4}$ in the two cases. This means that parameter D has a more linear relation with the refractive index than the other parameters. In part (c) of Figs. 4 and 5, the modified RA, exactly equal to parameters D, is compared with the conventional RA whose mathematical formula is given by Eq. (47). Lines of the conventional and modified RAs have a parallel relation with each other. All four lines in part (c) of Figs. 4 and 5 have linear correlation coefficients, r, of $1 - |r| < 10^{-4}$. The results of Figs. 4 and 5 indicate that the asymmetric SPR curve formula of Eq. (45) is very useful as a fitting function for the SPR curves. On the other hand, our theory shows that the modified RA is better in linearity than the conventional RA. In fact, the modified RA is better in linearity than the conventional RA by 1.9×10^{-5} for the linear correlation coefficient, while the modified and conventional RAs appear almost equal in linearity in Fig. 5c. This is an example that supports our theory.

Finally, the asymmetric SPR curve equation was examined by actual SPR experiments using sucrose solutions with the five concentrations of 0, 1, 4, 10 and 20 wt.%. The solid lines of part (a) in Figs. 6 and 7 were obtained by the SPR experiments with excitation wavelengths of 630 and 880 nm, respectively, while the broken lines are the fitting curves due to the asymmetric SPR curve equation. Table 3 shows two sets of five parameters obtained by fitting the SPR curves denoted by 0 wt.% in part (a) of Figs. 6 and 7. The experimental SPR curves largely differed from the theoretical SPR curves because of the optical distortion due to the hemicylindrical prism and cylindrical lens, spectral line broadening of the light source, the adhesive thin metal layer, and so on. In spite of that, the fitting curves closely agreed with the experimental SPR curves in Figs. 6a and 7a. This, therefore, suggests that close fits to the experimental SPR curves are impossible with less than five parameters while fits with more than five parameters give meaningless information on the SPR curves. Part (b) of Figs. 6 and 7 shows plots of the modified RA equal to parameter D and the conventional RA as a function of refractive indices of the sucrose solutions that are values at a temperature of 20 °C and at a wavelength of 589 nm [13]. Although the

Table 1
Actual coefficients of A, B, C, D and E used for the normalization in Figs. 4b and 5b (the coefficients are obtained when the refractive index of the sensing layer is 1.333)

	A	B	C	D	E
Fig. 4b	0.8798	3.066	0.8800	55.26	1.808
Fig. 5b	0.8939	0.1691	0.2015	50.39	0.4311

Table 2
Linear correlation coefficients of A, B, C, D and E with respect to the refractive index in Figs. 4b and 5b

	A	B	C	D	E
Fig. 4b	−0.99827	0.99919	0.99307	0.99995	0.99954
Fig. 5b	−0.99036	0.99897	0.98282	0.99998	0.99731

Table 3
Coefficients of A, B, C, D and E used for fitting SPR curves denoted by 0 wt.% in Figs. 6a and 7a

	A	B	C	D	E
Fig. 6a (0 wt.%)	0.7207	1.382	1.078	53.70	1.612
Fig. 7a (0 wt.%)	0.8527	0.1006	0.2054	49.24	0.6428

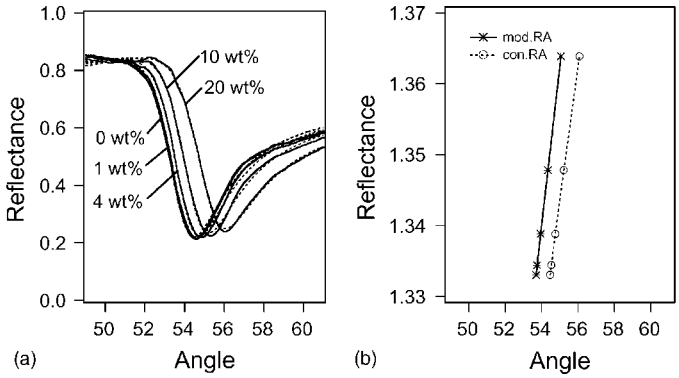

Fig. 6. Experimental examination of the asymmetric SPR curve equation by fitting of the SPR curves obtained at an excitation wavelength of 630 nm. Sucrose solutions with concentrations of 0, 1, 4, 10 and 20 wt.% are measured: (a) The solid lines are the experimental SPR curves while the broken lines are fitted to the asymmetric SPR curve equation given by Eq. (45). Parameters used for fitting SPR curves denoted by 0 wt.% are shown in Table 3. (b) Responses to refractive index changes of the mod.RA and con.RA. The mod.RA is given as parameter D by fitting to the asymmetric SPR equation. The con.RA is given as $D + (-B + \sqrt{B^2 + C^2E^2})/C$ in Eq. (47) by the fitting.

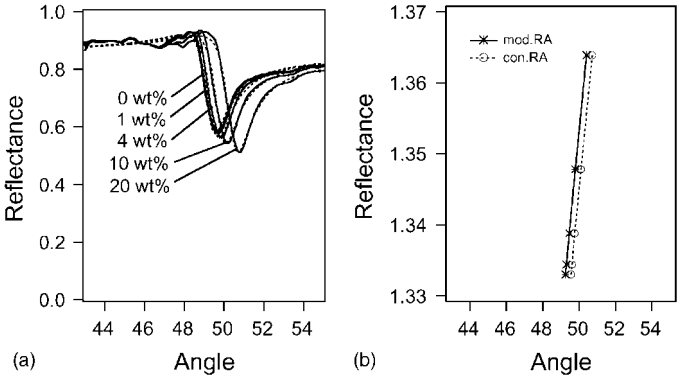

Fig. 7. Experimental examination of the asymmetric SPR curve equation by fitting of the SPR curves obtained at an excitation wavelength of 880 nm. Sucrose solutions with concentrations of 0, 1, 4, 10 and 20 wt.% are measured: (a) The solid lines are the experimental SPR curves while the broken lines are fitted to the asymmetric SPR curve equation given by Eq. (45). Parameters used for fitting SPR curves denoted by 0 wt.% are shown in Table 3. (b) Responses to refractive index changes of the mod.RA and con.RA determined by fitting to the asymmetric SPR equation.

measurement conditions are different in wavelength from the referred data [13], the relative changes in the refractive index of the sucrose solutions relative to that of water are almost the same irrespective of the wavelength. In Figs. 6b and 7b, the modified RA is better in linearity than the conventional RA by 2.0×10^{-4} and 1.4×10^{-4} for the linear correlation coefficient, respectively. In our case, there is a minor difference between the modified and conventional RAs, but in the high-performance SPR sensors, the modified RA would be more useful than the conventional RA.

Further experimental results and discussion will be required for proving the practical usefulness of the asymmetric SPR curve-fitting equation, though the numerical simulations in Figs. 2–5 and the experimental analyses in Figs. 6 and 7 are demonstrated. An important issue for discussing the practical usefulness of the asymmetric SPR curve-fitting equation is the real-time monitoring, which is planned for experiments and will be described elsewhere. Also, the asymmetric SPR curve-fitting equation is useful for SPR curves of absorption-based SPR sensors [14–16] that monitor changes in a complex refractive index caused by absorption changes. The asymmetric SPR curve-fitting equation is open for every real-time SPR sensory system personally developed or commercially available.

6. Conclusions

The proposed asymmetric SPR curve equation offers a powerful fitting function for real-time SPR sensors in terms of close fits to almost all SPR curves experimentally obtained. The new curve-fitting equation has only five parameters of the fits to be suitable for a fast procedure in computer-assisted real-time monitoring. The new equation has a theoretical background of a closer approximation of the three-layer Fresnel equation regarding p-polarization

than Kretschmann's SPR curve equation. It is theoretically found that the modified RA defined as parameter D in the proposed equation is a better parameter in monitoring refractive index changes than the conventional RA presenting the reflectance minimum in the SPR curve. The usefulness of the new equation in the fits to SPR curves was numerically and experimentally demonstrated.

Acknowledgements

We thank Dr. O. Niwa of the NTT Lifestyle and Environmental Technology Laboratories, Mr. T. Tobita of the NTT Advanced Technology Corporation and Mr. H. Hashimoto of the Airport Environment Improvement Foundation for their cooperation in the SPR experiments. Special thanks also go to Dr. Y. Iwasaki of the NTT Lifestyle and Environmental Technology Laboratories for fruitful discussions about the asymmetric SPR curve-fitting equation.

References

[1] J.R. Sambles, G.W. Bradbery, F. Yang, Contemp. Phys. 32 (1991) 173–183.
[2] J. Homora, S.S. Yee, G. Gauglitz, Sens. Actuators B 54 (1999) 3–15.
[3] http://www.biacore.com/.
[4] E. Kretschmann, Z. Physik 241 (1971) 313–324.
[5] K.S. Johnston, S.S. Yee, K.S. Booksh, Anal. Chem. 69 (1997) 1851–1884.
[6] K.S. Johnston, K.S. Booksh, T.M. Chinowsky, S.S. Yee, Sens. Actuators B 54 (1999) 80–88.
[7] T.M. Chinowsky, L.S. Jung, S.S. Yee, Sens. Actuators B 54 (1999) 89–97.
[8] I. Pockrand, Surf. Sci. 72 (1978) 577–588.
[9] W.P. Chen, J.M. Chen, Surf. Sci. 91 (1980) 601–617.
[10] W.P. Chen, J.M. Chen, J. Opt. Soc. Am. 71 (1981) 189–191.
[11] W.H. Press, B.P. Flannery, S.A. Teukolsky, W.T. Vetterling (Eds.), Numerical Recipes in C, Cambridge University Press, Cambridge, 1988.
[12] R.A. Innes, J.R. Sambles, J. Phys. F 17 (1987) 277–287.
[13] D.R. Lide (Ed.), Handbook of Chemistry and Physics, CRC Press, Boca Raton, FL, 1996.
[14] K. Kurihara, E. Hirayama, K. Nakamura, S. Sasaki, D. Citterio, K. Suziki, Proc. Pittcon 2000 (2000) 1323.
[15] K. Kurihara, K. Nakamura, E. Fujii, H. Hashimoto, D. Citterio, K. Suzuki, Proc. Pacifichem. 2000 (2000) 139.
[16] K. Kurihara, K. Suzuki, Anal. Chem. 74 (2002) 696–701.

Biographies

Kazuyoshi Kurihara received his BS and DS degrees in physics from the University of Tokyo in 1989 and 1994, respectively. He joined the photon control project of Kanagawa Academy of Science and Technology (KAST) from 1994 to 1998. He has worked for Collaboration of Regional Entities for the Advancement of Technological Excellence (CREATE) in KAST since 1999. His current work involves the development of new SPR instruments for chemical and biochemical sensing.

Kaori Nakamura received her BE degree in 2000 from Keio University. She is now a master course student in the same university. Her current interest is the development of absorption-based SPR sensors for chemical and biochemical sensing.

Koji Suzuki received his BE and DE degrees from Keio University in 1977 and 1982, respectively. He is Professor in Keio University as well as group leader of CREATE in KAST. His major is analytical chemistry with chemical and biochemical sensing/sensors.